Naval Research Laboratory

Washington, DC 20375-5000

NRL Memorandum Report 6549

A Solvable Self-Similar Model of the Sausage Instability in a Resistive Z-Pinch

MARTIN LAMPE

Beam Physics Branch
Plasma Physics Division

September 20, 1989

SECURITY CLASSIFICATION OF THIS PAGE

REPORT DOCUMENTATION PAGE

Form Approved
OMB No 0704-0188

1a REPORT SECURITY CLASSIFICATION UNCLASSIFIED	1b RESTRICTIVE MARKINGS
2a SECURITY CLASSIFICATION AUTHORITY	3 DISTRIBUTION/AVAILABILITY OF REPORT Approved for public release; distribution unlimited.
2b DECLASSIFICATION/DOWNGRADING SCHEDULE	
4 PERFORMING ORGANIZATION REPORT NUMBER(S) NRL Memorandum Report 6549	5 MONITORING ORGANIZATION REPORT NUMBER(S)
6a NAME OF PERFORMING ORGANIZATION Naval Research Laboratory 6b OFFICE SYMBOL (If applicable) Code 4790	7a NAME OF MONITORING ORGANIZATION
6c ADDRESS (City, State, and ZIP Code) Washington, DC 20375-5000	7b ADDRESS (City, State, and ZIP Code)
8a NAME OF FUNDING/SPONSORING ORGANIZATION Office of Naval Research 8b OFFICE SYMBOL (If applicable)	9 PROCUREMENT INSTRUMENT IDENTIFICATION NUMBER
8c ADDRESS (City, State, and ZIP Code) Arlington, VA 22217	10 SOURCE OF FUNDING NUMBERS PROGRAM ELEMENT NO / PROJECT NO: ONR / TASK NO / WORK UNIT ACCESSION NO

11 TITLE (Include Security Classification)

A Solvable Self-Similar Model of the Sausage Instability in a Resistive Z-Pinch

12 PERSONAL AUTHOR(S)
Lampe, Martin

13a TYPE OF REPORT	13b TIME COVERED	14 DATE OF REPORT (Year, Month, Day)	15 PAGE COUNT
Interim	FROM _____ TO _____	1989 September 20	38

16 SUPPLEMENTARY NOTATION

17 COSATI CODES		
FIELD	GROUP	SUB-GROUP

18 SUBJECT TERMS (Continue on reverse if necessary and identify by block number)
Z-pinch; Sausage instability; Pinch; MHD instability

19 ABSTRACT (Continue on reverse if necessary and identify by block number)

A solvable model is developed for the linearized sausage mode within the context of resistive MHD. The model is based on the assumption that the fluid motion of the plasma is self-similar, as well as several assumptions pertinent to the long-wavelength limit. The perturbations to the magnetic field are not assumed to be self-similar, but rather are calculated. Effects arising from time dependences of the equilibrium, e.g., current rising as t^{α}, ohmic heating, and time variation of the pinch radius, are included in the analysis. The formalism appears to provide a good representation of those modes that involve coherent sausage distortion of the entire cross section of the pinch, but excludes modes that are localized radially, and higher radial eigenmodes. For this and other reasons, it is expected that the model underestimates the maximum

(Continues)

20 DISTRIBUTION/AVAILABILITY OF ABSTRACT	21 ABSTRACT SECURITY CLASSIFICATION
☒ UNCLASSIFIED/UNLIMITED ☐ SAME AS RPT ☐ DTIC USERS	UNCLASSIFIED
22a NAME OF RESPONSIBLE INDIVIDUAL Martin Lampe	22b TELEPHONE (Include Area Code) (202) 767-4041 22c OFFICE SYMBOL Code 4792

DD Form 1473, JUN 86 *Previous editions are obsolete.* SECURITY CLASSIFICATION OF THIS PAGE

S/N 0102-LF-014-6603

19. ABSTRACTS (Continued)

instability growth rates, but is reasonable for global sausage modes. The net effect of resistivity and time variation of the equilibrium is to decrease the growth rate if $\alpha \lesssim 1$, but never by more than a factor of about two. The effect is to increase the growth rate if $\alpha \gtrsim 1$.

CONTENTS

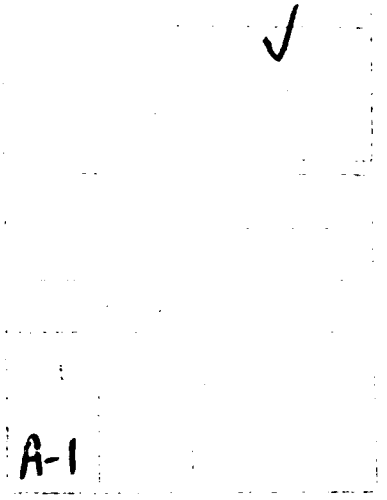

A SOLVABLE SELF-SIMILAR MODEL OF THE SAUSAGE INSTABILITY IN A RESISTIVE Z-PINCH

I. Introduction

Since the early days of controlled fusion research, it has been generally accepted that simple Z-pinches are violently unstable to both the sausage and kink modes. Specifically, ideal MHD unequivocally predicts instability for a time-independent pinch surrounded by vacuum, with growth rate of the order of kv_A for $ka_o \leq 1$, where k is the axial wave number, a_o is the equilibrium pinch radius, and v_A is the Alfven speed. The early experiments were indeed observed to be strongly unstable, in general agreement with this picture. These conclusions have, over the years, suppressed interest in the Z-pinch as a quiescent plasma confinement geometry, and apparently have also discouraged theoretical investigation of the stability problem from a more sophisticated point of view, e.g., with the inclusion of dissipative and kinetic effects, as well as those effects arising from time dependence of the equilibrium state.

However, recent experiments with deuterium-fiber-initiated Z-pinches at NRL[1] and Los Alamos[2] exhibit apparent stability over a very large number of Alfven growth times a_o/v_A. For example, in the NRL experiment, the pinch was apparently stable over the entire duration of the current rise, which is typically 130 ns but has been varied down to 110 ns to test sensitivity to this parameter. The pinch then goes sausage unstable after peak current is reached. Robson[1] has suggested that the stability is a direct consequence of rising current - the "$\dot{I}$ hypothesis". These observations have prompted a number of theoretical efforts to re-examine stability, with the emphasis being on the sausage mode, since the kink mode is not seen at all in the recent experiments. These recent and ongoing efforts include linearized one-dimensional (radial) treatments which assume a mode structure exp(ikz) and model the plasma either with resistive MHD,[3] or MHD with the full Braginskii transport coefficients,[4] or Chew-

Manuscript approved August 14, 1989.

Goldberger-Low,[5,6] or Vlasov ions.[7] In addition, there have been two-dimensional nonlinear fluid simulations that include resistivity[8] or full Braginskii transport,[4] or even the ongoing ablation of the deuterium fiber.[9] Preliminary results from some of this work has suggested that resistivity could be a significant stabilizing factor.[3,6] All of these treatments are essentially numerical, and do not provide analytic scaling laws, nor direct insights into the precise nature of stabilizing mechanisms. Also, these stability calculations have in most cases assumed time dependence $(t/t_o)^{1/3}$ for the current $I(t)$, which simplifies and restricts the problem by leading to a time-independent pinch radius.[10,11]

In this work we investigate the resistive MHD sausage linear stability problem, using an alternative approach which has the virtues of simplicity and generality, and directly provides analytic scaling laws as well as insight into physical mechanisms. We develop a model that admittedly includes some features that are not strictly correct, but which we expect to be at least reasonable. The model is motivated by those features appropriate to long-wavelength modes, but one hopes that it applies qualitatively for ka_o up to order unity. The principal assumptions are as follows: (i) The plasma temperature $T(r,z,t)$ is assumed to be independent of r, in both the equilibrium and the perturbation. (ii) Self-similar equilibria are investigated with $I(t) \propto (t/t_o)^{\alpha}$, where α can be any number. (iii) No heat transport along z is included in the investigations to date (but this could easily be included, and would be destabilizing). (iv) Radial pressure balance, i.e., the Bennett pinch condition,[12,13] is assumed in both the equilibrium and the perturbation. (v) The current $I(z,t)$ is assumed to be unchanged by the perturbation, and thus independent of z. (vi) Some terms of order $k^2a_o^2$ are dropped for convenience. (vii) The fluid motion of the sausaging is assumed to be self-similar. However,

the magnetic field $B(r,z,t)$ is not assumed to be self-similar, but rather is calculated from resistive MHD. With these assumptions, we are able to obtain an analytic solution for the growth of sausage perturbations.

In undertaking this calculation, we had in mind two particular resistive effects which, coupled to increasing $I(t)$, could be stabilizing. The first is that, according to the Bennett relation, the necks of the sausages must be hotter, and therefore less resistive, than the bulges; thus, if $\dot{I} > 0$, the skin effect is enhanced in the necks and (under some circumstances) the current in the necks is concentrated in a smaller fraction of the pinch area at the outside. This would reduce, at the necks, the magnetic pressure in the interior which pushes plasma axially out of the necks and thus drives the instability. The second effect is that (under some circumstances) ohmic energy dissipation is enhanced at the necks, where the plasma is compressed, and reduced at the bulges. This can be interpreted mathematically as an effective decrease in the plasma compressibility, i.e., an increase in the adiabatic index from its actual value 5/3, as regards the perturbation. We have calculated these and other resistive effects fully self-consistently, within the model described above. We find that if $\alpha \leq 1$, the growth rate is reduced, but not by more than about a factor of two, from the well-known value from ideal MHD with an assumed time-independent equilibrium.[14] In fact, there are other resistive terms which are destabilizing (as was recognized by R. J. Tayler[15] many years ago), and also some geometric terms associated with the time variation of the equilibrium radius if $\alpha \neq 1/3$. If $\alpha \geq 1$, the net result is that the growth rate is larger than the value from ideal MHD with a time-dependent equilibrium. Our model also can be interpreted as representing a plasma with large shear viscosity. Thus, it appears that within the context of a linearized fluid treatment neither resistivity nor

shear viscosity can account for the long period of stability observed in the deuterium-fiber experiments.

II. Self-Similar Equilibrium

The "equilibrium" state of the pinch is, in general, time-dependent, since I(t) will have a (specified) time dependence and the pinch will heat up resistively and expand or contract to maintain radial pressure balance. However, by definition, the equilibrium is z-independent. We assume radial pressure balance is maintained, and that the equilibrium is isothermal and has equal electron and ion temperatures. (However, all the conclusions also follow if $T_e \gg T_i$ or if T_e/T_i is a fixed ratio.) We also assume that the conductivity

$$\sigma \propto T^{3/2}, \tag{1}$$

in accordance with the Spitzer formula[13] with the variation of the Coulomb logarithm neglected, so that σ_o is also uniform within the plasma. The continuity, radial momentum, and magnetic diffusion equations are then

$$\frac{\partial \rho_o}{\partial t} + \frac{1}{r}\frac{\partial}{\partial r} r v_{ro} \rho_o = 0, \tag{2}$$

$$\frac{\partial P_o}{\partial r} + \frac{\partial}{\partial r}\frac{B_o^2}{8\pi} = -\frac{B_o^2}{4\pi r}, \tag{3}$$

$$\frac{\partial B_o}{\partial t} = -\frac{\partial}{\partial r} v_{ro} B_o - \frac{c^2}{4\pi\sigma_o}\frac{\partial}{\partial r}\frac{1}{r}\frac{\partial}{\partial r} r B_o, \tag{4}$$

where ρ is the density, P the pressure, v_r the radial velocity, and subscript-zero denotes equilibrium. There is also an energy equation which we will write down later in radially-integrated form.

It is well known[10,11,16] that these equations admit a self-similar solution, defined by the relations

$$x = \frac{r}{a_o(t)}, \tag{5}$$

$$v_{ro} = \dot{a}_o(t)x, \tag{6}$$

$$\rho_o(r,t) = \frac{N_o m_i}{\pi a_o^2(t)} \hat{\rho}_o(x), \tag{7}$$

$$B_o(r,t) = \frac{2I(t)}{ca_o(t)} \hat{B}_o(x), \tag{8}$$

$$J_o(r,t) = \frac{I(t)}{\pi a_o^2(t)} \hat{J}_o(x) = \frac{c}{4\pi} \frac{1}{r} \frac{\partial}{\partial r} rB_o(r,t), \tag{9}$$

where $a_o(t)$ is the pinch outer radius, N_o is the number of ions per unit length, and m_i is the ion mass.

Equation (2) is automatically satisfied by (5) - (7). Equation (3) implies the Bennett relation,

$$T_o = \frac{I^2}{4N_o c^2}, \tag{10}$$

where the temperature T is in ergs. Beyond that, we shall not need to solve (3) for the pressure P_o. Equation (4) reduces to a Bessel equation,

$$\frac{\partial}{\partial x} \frac{1}{x} \frac{\partial}{\partial x} x \hat{B}_o + \frac{4\pi\sigma_o a_o^2}{c^2} \frac{\dot{I}}{I} \hat{B}_o = 0, \tag{11}$$

to which the solution [normalized to unity at x = 1 as required by (8)] is

$$\hat{B}_o(x) = \begin{cases} \dfrac{I_1(qx)}{I_1(q)} & , \ 0 \le x \le 1 \qquad (12a) \\ x^{-1} & , \ 1 \le x \qquad (12b) \end{cases}$$

where I_1 is a modified Bessel function and

$$q^2 \equiv \frac{4\pi\sigma_o(t)a_o(t)}{c^2}\,\frac{\dot{I}(t)}{I(t)}. \tag{13}$$

However, we have assumed $\hat{B}_o(x)$, and therefore q, to be time-independent. This can be satisfied if

$$I(t) = I_o(t/t_o)^{\alpha}, \tag{14}$$

in which case (1) and (10) imply

$$\sigma_o(t) \propto (t/t_o)^{3\alpha}, \tag{15a}$$

and thus it is required that

$$a_o(t) \propto (t/t_o)^{(1-3\alpha)/2} \tag{15b}$$

so that

$$q^2 = \frac{\alpha}{t}\,\frac{4\pi\sigma_o a_o^2}{c^2} \tag{16}$$

is indeed time-independent.

The energy equation, including both ohmic and compressional heating and assuming an ideal gas with adiabatic index 5/3, is

$$3\,N_o\dot{T}_o + \frac{4\dot{a}_o}{a_o}\,N_oT_o = \frac{1}{\sigma_o}\int_0^{a_o} dr\; 2\pi r\; J_o^2. \tag{17}$$

Using the Bennett relation (10) to eliminate T_o, Eqs. (9), (12) and (13) to determine $J_o(r,t)$, and Eqs. (14) and (15b) to specify $\dot{I}/I$ and $\dot{a}_o/a_o$, Eq. (17) reduces to an equation that determines q as a function of α:

$$4\alpha = \frac{I_1^2(q)}{\int_0^1 dx\, x\, I_o^2(qx)}. \tag{18}$$

Equation (18) is plotted in Fig. 1. In the limiting cases of small and large α, the Bessel functions can be expanded and we find

$$q \simeq \begin{cases} \sqrt{8\alpha}\ , & \alpha \leq 1 \quad (19a) \\ 2\alpha\ , & \alpha >> 1 \quad (19b) \end{cases}$$

Also, in the case $\alpha = 1/3$ which corresponds to a fixed radius a_o,

$$q(\alpha = 1/3) = 1.65 \tag{19c}$$

Recently, Rosenau, Nebel and Lewis[17] have shown numerically that the self-similar solutions are stable, and are attractors for a broad class of initial conditions, as long as the pinch is legislated mathematically to be uniform in z.

In this paper, we shall apply our perturbation model to this particular equilibrium. However, the perturbation analysis is more general, and could be applied to other assumed equilibria. We have in fact, as a check on the perturbation model, used it to calculate ideal MHD growth rates for various assumed time-independent equilibria, but these calculations will not be presented here.

III. Linearized Perturbation Analysis

In the present section, we allow all quantities to depend on z as well as r and t, except that we specify that I(t) is z-independent so as to prevent charge accumulation anywhere in the pinch. We shall soon specialize to the case of small departures from a z-independent equilibrium, but we begin by writing down the nonlinear equations for continuity, momentum, energy, and magnetic field diffusion. With long wavelength perturbations in mind, we continue to assume that radial pressure balance is satisfied, and that T(r,z,t) is independent of r but that there is no heat conduction along z. The basic equations then are:

$$\frac{\partial \rho}{\partial t} + \frac{\partial}{\partial z}(\rho v_z) + \frac{1}{r}\frac{\partial}{\partial r} r\rho v_r = 0, \tag{20}$$

$$\frac{\partial}{\partial r}\left(P + \frac{B^2}{8\pi}\right) = -\frac{B^2}{4\pi r}, \tag{21}$$

$$\rho \frac{\partial v_z}{\partial t} = -\frac{\partial}{\partial z}\left(P + \frac{B^2}{8\pi}\right), \tag{22}$$

$$\frac{\partial B}{\partial t} + \frac{\partial}{\partial r}\left(v_r B\right) + \frac{\partial}{\partial z}\left(v_z B\right) = \frac{c^2}{4\pi\sigma}\frac{\partial}{\partial r}\frac{1}{r}\frac{\partial}{\partial r} rB + \frac{c^2}{4\pi}\frac{\partial}{\partial z}\frac{1}{\sigma}\frac{\partial B}{\partial z}. \tag{23}$$

Now we make the key simplification that allows us to develop a solvable model: we require the fluid motion to be radially self-similar, i.e., that $\rho(r,z,t)$ be of the form

$$\rho(r,z,t) = \frac{N(z,t)m_i}{\pi a^2(z,t)}\,\tilde{\rho}(x,z), \tag{24a}$$

where N(z,t) is the perturbed number of ions per unit length, a(z,t) is the perturbed outer radius of the pinch, and now

$$x \equiv r/a(z,t). \tag{25}$$

This is equivalent to specifying that

$$v_r(r,z,t) = x \frac{\partial}{\partial t} a(z,t), \tag{24b}$$

$$v_z(r,z,t) = v_z(z,t), \text{ independent of } r. \tag{24c}$$

We have seen that self-similar forms were exact solutions for the equilibrium, but Eqs. (24) are not in general exact solutions of the z-dependent perturbation equations; they are imposed externally to specify our model. However, we regard them as a qualitatively reasonable representation, particularly in the long-wavelength limit, which is the focus of our study, for the class of sausage perturbations that are readily observed experimentally and that are expected to be most disruptive - i.e., those that consist of a more or less coherent pinching of the entire plasma cross-section at the "necks", and expansion of the entire cross-section at the bulges. Our model excludes modes which are strongly localized to a limited shell in r, and higher radial modes which may have parts of the plasma cross-section moving inward at the same time when other parts are moving outward. In some cases, particularly within ideal MHD, these types of modes may have the largest linear growth rates, but one does not expect them to have the same type of disruptive effect, when they reach large amplitude, as the global sausage modes. Since we are excluding certain classes of modes, in general, we expect our model to yield linear growth rates which are somewhat less unstable than the exact results of resistive MHD, but to yield qualitatively accurate growth rates for any global modes that are present. Indeed, we have tested the model by applying it with zero resistivity to some simple time-independent equilibria, and found this to be the case.

It is also worth noting that Eq. (24c), which is equivalent in itself to the self-similar assumption, becomes exact in the limit of long wavelength and large shear viscosity. Thus, the present model becomes a true representation of the physics in that limit.

The inexactness of the model becomes clear when Eq. (22) is solved; in general, the solution will be of a value of v_z that varies with r, contradicting Eq. (24c). Thus, to make our model self-consistent, we set v_z equal to the <u>average</u> value given by (22), i.e., we replace (22) with

$$Nm_i \frac{\partial v_z}{\partial t} = - \frac{\partial}{\partial z} \int_0^a dr\ 2\pi r \left(P + \frac{B^2}{8\pi}\right). \tag{26}$$

We now add an energy equation to complete our set of nonlinear fluid equations:

$$\frac{\partial}{\partial t}\left(3\ NT\right) + \frac{\partial}{\partial z}\left(3\ NTv_z\right) + \left(2\frac{\dot{a}}{a} + \frac{\partial v_z}{\partial z}\right) 2\ NT = \frac{1}{\sigma(z,t)} \int_0^a dr 2\pi r J^2(r,z,t). \tag{27}$$

However, we can simplify (27) by using the Bennett relation,

$$N(z,t)\ T(z,t) = \frac{I^2(t)}{4c^2}, \tag{28}$$

which follows from (21). We have assumed

$$I(z,t) = I(t) \tag{29}$$

to be independent of z. Then (27) becomes

$$\frac{3\dot{I}}{I} + \left(2\frac{\dot{a}}{a} + \frac{5}{2}\frac{\partial v_z}{\partial z}\right) = \frac{2c^2}{I^2\sigma} \int_0^a dr 2\pi r J^2(r,z,t). \tag{30}$$

Now we linearize our basic set of Eqs. (20), (21), (23), (28), and (30), by defining

$$\frac{a(z,t)}{a_o(t)} = 1 + \hat{a}, \tag{31a}$$

$$\frac{\sigma(z,t)}{\sigma_o(t)} = 1 + \hat{\sigma}, \tag{31b}$$

$$\frac{N(z,t)}{N_o(t)} = 1 + \hat{N}, \tag{31c}$$

$$I(t) = I_o(t), \tag{31d}$$

$$B(r,z,t) = \frac{a_o}{a} B_o\left(\frac{a_o}{a} r, t\right) + \frac{2I}{ca} \hat{B}(x,z,t), \tag{32a}$$

$$J(r,z,t) = \left(\frac{a_o}{a}\right)^2 J_o\left(\frac{a_o}{a} r, t\right) + \frac{I}{\pi a^2} \hat{J}(x,z,t). \tag{32b}$$

Equations (32) define the first-order quantities $\hat{B}$ and $\hat{J}$ in terms of the difference between the exact values $B(r,z,t)$, $J(r,z,t)$ and self-similar forms that carry the same current. This somewhat unusual approach is very convenient for handling the boundary conditions at $r = a$, where both $J(r,z,t)$ and $\sigma(r,z,t)$ jump discontinuously to zero. With the definitions (32) and using x rather than r as our independent variable, all discontinuities occur exactly at $x = 1$, it is not necessary to add any surface terms to the first-order equations, and the boundary conditions are

$$\hat{B}(0,t) = 0, \tag{33a}$$

$$\hat{B}(x,t) = 0, \text{ for } x \geq 1, \tag{33b}$$

$$\hat{J}(x,t) = 0, \text{ for } x > 1. \tag{33c}$$

Note that $\hat{J}$ is, in general, discontinuous at $x = 1$, but if σ is finite $\hat{B}$ is continuous.

We treat all quantities with carets as first-order small quantities with z-dependence exp(ikz), neglect second order, and also define

$$\hat{v} = ikv_z. \tag{34}$$

Then Eq. (20) reduces to

$$\frac{d\hat{N}}{dt} = -\hat{v}. \tag{35}$$

Equations (28), (31d), and (35) give

$$\frac{d\hat{T}}{dt} = \hat{v}, \tag{36}$$

and continuing to use $\sigma \propto T^{3/2}$, we have

$$\frac{d\hat{\sigma}}{dt} = \frac{3}{2}\hat{v}. \tag{37}$$

It is useful to explicitly expand Eqs. (32) to first order, using (8) and (9)

$$B(r,t) = \frac{2I}{ca_o}\left[(1 - \hat{a})\,\hat{B}_o(x) + \hat{B}(x,t)\right], \tag{38a}$$

$$J(r,t) = \frac{I}{\pi a_o^2}\left[(1 - 2\hat{a})\,\hat{J}_o(x) + \hat{J}(x,t)\right]. \tag{38b}$$

We integrate (21), using (38), (12b), and (33b), to obtain

$$P + \frac{B^2}{8\pi} = \int_r^\infty \frac{dr' B^2(r')}{4\pi r'}$$

$$= \frac{I^2}{\pi c^2 a_o^2}\left[(1 - 2\hat{a})\left(\frac{1}{2} + \int_x^1 \frac{dx'}{x'}\hat{B}_o^2(x') + 2\int_x^1 \frac{dx'}{x'}\hat{B}_o(x')\hat{B}(x')\right]. \tag{39}$$

We now use this in the equation of motion (26). Reversing the order of integrations and explicitly using (12) for the equilibrium field, we obtain

$$\frac{d\hat{v}}{dt} = \frac{2k^2I^2}{N_o m_i c^2}\left[-\hat{a}\left(\frac{1}{2} + \int_0^1 \frac{dx x I_1^2(qx)}{I_1^2(q)}\right) + \int_0^1 \frac{dx x I_1(qx)\hat{B}(x)}{I_1(q)}\right]. \quad (40)$$

After some algebra but no further approximations, the magnetic field Eq. (23) can be put in the form

$$\left(\frac{\partial}{\partial t} + \frac{\alpha}{t} - \frac{c^2}{4\pi\sigma_o a_o^2}\frac{\partial}{\partial x}\frac{1}{x}\frac{\partial}{\partial x}x + \frac{k^2c^2}{4\pi\sigma_o}\right)\hat{B}$$

$$= \left[\frac{\alpha}{t}\hat{a} - \hat{v} - \frac{\alpha}{t}(\hat{\sigma} + 3\hat{a}) + \frac{k^2c^2}{4\pi\sigma_o}\hat{a}\right]\frac{I_1(qx)}{I_1(q)}. \quad (41)$$

Finally, the ohmic heating term in (30) can be calculated in linearized form and the energy equation put in the form

$$\frac{d\hat{a}}{dt} = -\frac{5}{4}\hat{v} - \frac{1-3\alpha}{2t}A - \frac{c^2}{4\pi\sigma_o a_o^2}\left[\frac{q^2}{2\alpha}(\hat{\sigma} - 2\hat{a}) + 4q^2\int_0^1 \frac{dx x I_1(qx)\hat{B}(x)}{I_1(q)}\right], \quad (42)$$

where we have explicitly used the time dependence (15b) of $a_o(t)$.

Equations (37), (40), (41), and (42) with the boundary conditions (33a,b) constitute a complete set of homogeneous equations for the time evolution of $\hat{\sigma}(t)$, $\hat{v}(t)$, $\hat{a}(t)$, and $\hat{B}(x,t)$. We clean up the equations a bit by dropping the k^2c^2 terms on each side of (41); these terms correspond to magnetic diffusion along z, and are stabilizing but small in the long wavelength limit. We also use (13) and (14) to eliminate σ_o in terms of q, and define a characteristic Alfven velocity v_A by

$$v_A^2 = \frac{B_o^2(a_o)}{4\pi\left(N_o m_i/\pi a_o^2\right)} = \frac{I^2}{N_o m_i c^2}. \quad (43)$$

Then Eqs. (40) - (42) become

$$\frac{d\hat{v}}{dt} = k^2 v_A^2 \left\{ - [1 + 2I_{11}(q)]\, \hat{a} + 2 \int_0^1 \frac{dx x I_1(qx) \hat{B}(x,t)}{I_1(q)} \right\}, \qquad (44)$$

$$\frac{d\hat{a}}{dt} = - \frac{5}{4} v - \frac{1-3\alpha}{2t} \hat{a} - \frac{\hat{a}}{t} - \frac{\hat{\sigma}}{2t} - \frac{4\alpha}{t} \int_0^1 \frac{dx x I_1(qx) \hat{B}(x,t)}{I_1(q)}, \qquad (45)$$

$$\left(\frac{\partial}{\partial t} + \frac{\alpha}{t} - \frac{\alpha}{q^2 t} \frac{\partial}{\partial x} \frac{1}{x} \frac{\partial}{\partial x} x \right) \hat{B}(x,t) = \left[- \hat{v} - \frac{\alpha}{t} (\hat{\sigma} + 2\hat{a}) \right] \frac{I_1(qx)}{I_1(q)}, \qquad (46)$$

where

$$I_{11}(q) \equiv \frac{\int_0^1 dx x I_1(qx)}{I_1^2(q)}. \qquad (47a)$$

The quantity I_{11}, which can be regarded as a function of α, is shown in Fig. 1. Using (18) and doing some integrations by parts, we can write

$$I_{11} = \frac{I_0(q)}{q I_1(q)} - \frac{1}{4\alpha}, \qquad (47b)$$

in which form it is clear that

$$I_{11}(0) = \frac{1}{4}, \quad \text{if } \alpha << 1, \qquad (48a)$$

$$I_{11}(\infty) = \frac{1}{4\alpha}, \quad \text{if } \alpha >> 1. \qquad (48b)$$

I_{11} is a monotonic decreasing function of α (i.e., of q) which is well approximated by

$$I_{11}(\alpha) \simeq \frac{1}{4(1+\alpha)}. \qquad (49)$$

The expression (49) is always smaller than the exact value of I_{11}, with the inaccuracy peaking at ~ 12% over a wide range of α from ~ 0.5 to ~ 3.

Before proceeding with the solution of Eqs. (37), (44) - (46), and (33), we shall pause to discuss the general nature of these equations and the origin and significance of their terms. If instability is present, in general, all time derivatives will be positive at times of primary interest (instability is non-oscillatory), as will be discussed. At a sausage neck, where $\hat{a} < 0$, we will find $\hat{v} > 0$ (plasma flowing out axially), and thus, $\hat{N} < 0$, and thus $\hat{\sigma} > 0$ (the neck must be hotter, according to the Bennett relation, and so has higher conductivity). The basic instability, which is familiar from ideal MHD analysis of a time-invariant equilibrium, is given by the first terms on the right-hand side (RHS) of (44) and (45); these yield a growth rate on the scale of kv_A, with some dependence on the equilibrium current profile through I_{11}. The last term of (44) represents the effect of non-self-similar evolution of B: typically J(r,z,t) will be more peaked at the outside of the pinch at a neck, i.e., $\hat{B}(x)$ for $0 < x < 1$ will be negative where $\hat{a} < 0$, which weakens the pressure pushing plasma out of the neck. Thus, this term is stabilizing. In Eq. (45), the term $(1-3\alpha)\hat{a}/2t$ arises simply from the fact that perturbations to a(z,t) must be scaled to a_o, which is itself a time-varying quantity; this geometric effect does have a significant effect on instability growth rates, as we shall see. The last three terms of (45) arise from the differences in ohmic heating between sausage necks and bulges: if there is extra heating at the necks, this is stabilizing by, in effect, increasing the adiabatic index (stiffness) of the plasma and opposing further shrinkage of the neck. The $\hat{a}/t$ term in (45) represents increase of ohmic heating at a neck due to self-similar compression of the current density; the $\hat{\sigma}/2t$ term represents decrease of ohmic heating due to increased conductivity; and the last term represents increased ohmic heating due to current concentration at the

outside resulting from departures from self-similarity. It remains to be determined under what circumstances the stabilizing terms win out.

Equation (46) shows the ways in which B(r) departs from self-similarity. The first term on the RHS represents decrease of B at a neck due to axial convection of B along with the outflowing plasma. The $\alpha(\hat{\sigma} + 2\hat{a})/t$ term represents the first-order contribution to the skin effect in a situation where $\dot{I} > 0$. As in the discussion of Eq. (45), the strength of the skin effect scales as the ratio of the magnetic diffusion time $4\pi\sigma_o a_o^2/c^2$ to the current rise time $I/\dot{I}$; hence, the first-order term scales as $\alpha(\hat{\sigma} + 2\hat{a})/t$. Clearly, these terms, which arise from the combined effect of resistivity and rising current, have the potential to be stabilizing, but must be evaluated to determine their effect.

IV. Solution of the Perturbation Equations

Equations (37), (44)-(46), and (33a,b) could be solved numerically, e.g., by using a Fourier-Bessel expansion of (46). However, as our objective here is to obtain analytic scaling laws in simple form, we choose to perform a simpler approximate analysis. We note that $\hat{B}(x,t)$ appears in Eqs. (44) and (45) only in the integral form

$$b(t) \equiv \int_0^1 \frac{dx x I_1(qx)\hat{B}(x,t)}{I_1(q)}. \tag{50}$$

Equation (46) for $\hat{B}$ has the particular solution

$$\hat{B}_1(x,t) = F(t)\,\frac{I_1(qx)}{I_1(q)}, \tag{51}$$

$$F(t) \equiv \int_{-\infty}^{t} dt' \left[\hat{v} + \frac{\alpha}{t}(\hat{\sigma} + 2\,\hat{a})\right]. \tag{52}$$

However, (51) fails to satisfy the boundary condition (33b), and thus, we must add in a homogeneous solution $B_2(x,t)$ with the correct boundary condition:

$$\hat{B}(x,t) = \hat{B}_1(x,t) + \hat{B}_2(x,t), \tag{53}$$

$$\left(\frac{\partial}{\partial t} + \frac{\alpha}{t} - \frac{\alpha}{q^2 t}\frac{\partial}{\partial x}\frac{1}{x}\frac{\partial}{\partial x}x\right)\hat{B}_2 = 0, \tag{54a}$$

$$\hat{B}_2(0,t) = 0, \tag{54b}$$

$$\hat{B}_2(1,t) = -F(t). \tag{54c}$$

We shall argue that over the time scale of primary interest to us, it is reasonable qualitatively to neglect B_2.

In general, we cannot produce a closed-form solution for $\hat{B}_2(x,t)$. But for the special case where

$$F(t) \propto t^{\eta}, \tag{55}$$

the solution to Eq. (54) is

$$\hat{B}_2(x,t) = -F(t)\,\frac{I_1(\sqrt{1+\eta/\alpha}\,qx)}{I_1(\sqrt{1+\eta/\alpha}\,q)}. \tag{56}$$

In this case, the integral b(t) of Eq. (50) can be written as a sum of contributions from $B_1(x,t)$ and $B_2(x,t)$:

$$b(t) = b_1(t) + b_2(t), \tag{57}$$

$$b_1(t) = F(t)\int_0^1 dx\,x\,\frac{I_1^2(qx)}{I_1^2(q)} \tag{58a}$$

$$b_2(t) = -F(t)\int_0^1 dx\,x\,\frac{I_1(qx)I_1(\sqrt{1+\eta/\alpha}\,qx)}{I_1(q)I_1(\sqrt{1+\eta/\alpha}\,q)}. \tag{58b}$$

If

$$\frac{\eta+\alpha}{\alpha} q^2 >> 1 , \tag{59a}$$

and also

$$\frac{\eta+\alpha}{\alpha} q^2 >> q^2, \tag{59b}$$

then $\hat{B}_2(x,t)$ is localized near $x = 1$ and as a result

$$b_2 >> b_1. \tag{60}$$

Conditions (59) are both satisfied if and only if

$$\eta q^2/\alpha >> 1. \tag{61}$$

In fact, b_2/b_1 is of order $(\alpha/\eta q^2)^{1/2}$. The interpretation of these equations is that if the perturbation grows rapidly enough compared to the equilibrium current-rise time scale, then $\hat{B}_2(x,t)$ is essentially a surface current perturbation, which does not have time to diffuse substantially into the pinch; this current contributes little to the integrated quantity $b(t)$ that occurs in (44) and (45).

If the time dependence of $F(t)$ is not a power law, we cannot solve for $\hat{B}_2(x,t)$ in closed form, but the same physical argument applies with η defined by

$$\eta = \frac{tF'(t)}{F(t)}. \tag{62}$$

If, for example, $F(t) \propto e^{\gamma t}$, the condition for neglecting B_2 is

$$\gamma t >> \alpha/q^2. \tag{63}$$

For the limiting cases of small and large α, we see from Eq. (19) that this reduces to

$$\gamma t >> \frac{1}{8} \text{ , if } \alpha << 1, \tag{64a}$$

or

$$\gamma t >> 1/4\alpha, \text{ if } \alpha >> 1. \tag{64b}$$

In either case, the criterion is well satisfied at a time when no more than one e-fold of unstable growth has occurred. We are generally interested in the longer time scale over which an instability e-folds several times, so it is reasonable to approximate $\hat{B}(x,t)$ by the particular solution $\hat{F}_1(x,t)$ whose x-dependence is known. We note from (51), (56) and (58) that this approximation increases $|b(t)|$, and this is true quite generally if $\dot{I} > 0$. The quantity b(t), i.e., the effect of the deviation of B(r,t) from self-similarity, is unambiguously stabilizing, as will be discussed below. Thus, the approximation of $\hat{B}(x,t)$ by $\hat{B}_1(x,t)$ reduces the growth rates which we shall calculate.

Referring to Eqs. (50) - (52), (57) and (58), we see that the partial differential equation (46) can now be replaced by an ordinary differential equation for b(t), so that (37), (44) - (46), and (33a,b) reduce to a set of four homogeneous first-order linear ordinary differential equations, which can be written in the matrix form

$$\frac{d}{dt}\begin{bmatrix} \dot{v} \\ \dot{a} \\ b \\ \dot{\sigma} \end{bmatrix} = -\begin{bmatrix} 0 & (1+2I_{11})k^2v_A^2 & -2k^2v_A^2 & 0 \\ 5/4 & 3(1-\alpha)/2t & 4\alpha/t & 1/2t \\ I_{11} & 2I_{11}\alpha/t & 0 & I_{11}\alpha/t \\ -3/2 & 0 & 0 & 0 \end{bmatrix}\begin{bmatrix} \dot{v} \\ \dot{a} \\ b \\ \dot{\sigma} \end{bmatrix} \tag{65}$$

The eigenvalues of this matrix give the instantaneous growth rate of perturbations; this growth rate will generally be time-varying, since the equilibrium varies with time, i.e., growth will not be purely exponential.

It is convenient to define Γ as the eigenvalue scaled to $kv_A(t)$. We then find the following quartic equation to determine the four eigenvalues:

$$0 = 4(kv_At)^2\Gamma^4 + 6(1-\alpha)kv_At\,\Gamma^3 - [(5+2I_{11})(kv_At)^2 + 32\alpha^2 I_{11}]\Gamma^2$$

$$+[-3+(6-4\alpha)I_{11} + 32\alpha I_{11}^2]kv_At\,\Gamma + 6(1+\alpha+8\alpha I_{11})\alpha I_{11}. \qquad (66)$$

The ideal MHD limit corresponds to $kv_At \to \infty$. (The temperature increases steadily as $T \propto I^2$, so resistivity becomes negligible at late times.) It is also possible to express kv_At as

$$kv_At = \frac{\alpha}{q^2}(ka_o)S, \qquad (67)$$

$$S \equiv \frac{4\pi\sigma_o(t)a_o^2(t)}{c^2}\frac{v_A(t)}{a_o(t)}, \qquad (68)$$

is the Lundquist number,[18] which has been used in the literature[3,8] as an indication of the strength of resistive effects. It is apparent from Eqs. (65) - (67) that the growth rate and other characteristics of the instability, for a given value of α, can depend on S and ka_o only as the combination $(ka_o)S$. S is a monotonically increasing function of time, and large S corresponds to the ideal MHD limit. In this limit, (66) gives

$$\Gamma = \left(\frac{5+2I_{11}}{4}\right)^{1/2}, \qquad (69)$$

i.e., growth is on the Alfven time scale, as expected. We may regard the four eigenvalues Γ_1, Γ_2, Γ_3 and Γ_4 as functions of kv_At. The eigenvalue that appears in Eq. (69), which we shall denote $\Gamma_1(kv_At)$, is always the largest and thus of primary interest. We have solved Eq. (66) for the value of Γ as a function of kv_At or equivalently of $(ka_o)S$. It is convenient to plot Γ_1 as a function of $(kv_At)^{-1}$, which is an indication of

the strength of non-ideal effects. The results are shown in Fig. 2. It is apparent that for $\alpha \ll 1$, the value of Γ_1 is reduced by non-ideal effects, but only to $\Gamma_1 = 1/2$ even for $\alpha \to 0$ in the limit $kv_A t \to 0$. For small finite values of α, e.g. the case $\alpha = 1/3$ shown in Fig. 2, Γ_1 decreases as a function of $(kv_A t)^{-1}$, but goes complex for times earlier than a finite value $kv_A t^*$. Thus, the instability is predicted to exhibit oscillatory growth for $t < t^*$. However, $t < t^*$ corresponds to less than one e-fold of growth, and our neglect of $\dot{B}_2(x,t)$ [Eqs. (53) - (58)] becomes questionable at these early times, so we do not plot the complex values of Γ_1. In no case do we find stability, or even reduction of the ideal MHD growth rate by more than about a factor of two, for time scales of interest.

For $\alpha \geq 1$, we find Γ_1 to be a rapidly increasing function of $(kv_A t)^{-1}$, i.e., the growth rate is much larger than the ideal MHD growth rate for a static equilibrium. Tracing back through the mathematics, we can see that this rapid growth is primarily due to the 2-2 matrix element of Eq. (65), i.e., to the term $(1-3\alpha)\dot{a}/2t$ on the RHS of Eq. (45) for $d\dot{a}/dt$. This is not a resistive effect, but simply a geometric one arising from the increasing $I(t)$, which is not balanced by enough ohmic heating to maintain pressure balance at constant pinch radius a_o. If $\alpha > 1/3$, the equilibrium radius $a_o(t)$ of the pinch steadily decreases as $t^{(1-3\alpha)/2}$, but any perturbations to the radius do not collapse as quickly. This effect tends to increase $\dot{a}(t) \equiv (a - a_o)/a_o$, which is the quantity that drives the growth of the perturbations. Additionally, because of this effect perturbations to σa^2 are dominated by the $2\dot{a}$ perturbation rather than the $\dot{\sigma}$ perturbation: hence the skin effect is <u>weaker</u> at a sausage neck, which is destabilizing, as discussed in Sec. III.

Concluding Remarks

We have used a self-similar model to calculate sausage mode growth rates within the framework of resistive MHD. Although our model is a simplification of the perturbation dynamics, it does treat quite a general class of time-dependent exact equilibria, it is fully self-consistent in its treatment of equilibrium and perturbations, and it is a fully resistive treatment from the outset rather than being a perturbative treatment of departures from ideal MHD. Furthermore, we expect the self-similar assumption to be at least qualitatively reasonable in calculating growth rates for global modes, and in any event to yield growth rates that are smaller than exact solutions of resistive MHD. Thus, it is disappointing that our results fail to explain the long-lived apparent stability of the recent deuterium-fiber Z-pinch experiments.[1,2] We do find reductions in the instability growth rate for the case $I \propto t^{1/3}$ where the equilibrium pinch radius is time-independent, and for other cases $I \propto t^{\alpha}$ with α small, but the reductions are by no more than a factor of two, which is insufficient to explain the experiments.

Assuming the experimental observations to be a valid indication of stability over a significant parameter regime, we may well ask what types of physical effects could account for this stability. Several types of effects come to mind, which have been excluded by the assumptions of the present model, and also by assumptions made in other recent calculations. First, we (and others) have assumed the current $I(z,t)$ to be z-independent and equal to the equilibrium current. If, in fact, $I(z,t)$ is reduced at the sausage necks - which would amount to some capacitive loading with charge accumulating on the shoulders of the sausages - that would have a stabilizing effect on the mode. Secondly, we (and others) have assumed the temperature within a given slice (i.e., at a given value of z) to be

independent of r. This is in agreement with the numerical equilibrium calculations of Lindemuth, et al[19] provided there is no remaining residual solid fiber. However, these authors argue that many tens of nanoseconds pass before the fiber is fully ablated, and find that the presence of the fiber at r = 0, which cools the plasma there, results in a ramped profile for T(r). It is possible that such a profile is more stable to sausage perturbations. We have not calculated either of these effects and merely suggest them as possible avenues for future investigation.

More generally, it should be noted that diagnostics used in the present generation of fiber z-pinch experiments would detect sausage instability only when it has reached large amplitude. Thus, it is possible that nonlinear effects excluded from the present linearized treatment, and possibly coupled to the effects of increasing current, resistivity, and other dissipative mechanisms may play a role in explaining the stability observed in the experiments.

Acknowledgments

The author is grateful to F. L. Cochran, A. E. Robson, M. Coppins, and I. D. Culverwell for discussions of work in progress. Some of the present work was inspired by previous calculations performed by these investigators. The author also has profited from conversations with D. Mosher. This work was performed in part while the author was a guest at the Laboratory for Plasma Research at the University of Maryland, whose hospitality is appreciated.

This work was supported by the Office of Naval Research.

References

1. J. D. Sethian, A. E. Robson, K. A. Gerber, and A. W. DeSilva, Phys. Rev. Lett. 59, 892 (1987); 59, 1790 (1987).
2. J. E. Hammel and D. W. Scudder, Proc. 14th European Conference on Controlled Fusion and Plasma Physics, Madrid, 1987, Contributed papers, Part 2, p. 450.
3. I. D. Culverwell, M. Coppins, and M. G. Haines, Second International Conference on High Density Pinches, Laguna Beach, CA, 1989, in press.
4. A. H. Glasser and R. A. Nebel, ibid.
5. M. Coppins, Phys. Fluids, in press.
6. M. Coppins and J. Scheffel, op. cit. Ref. 3.
7. T. D. Arber and M. Coppins, ibid.
8. F. L. Cochran and A. E. Robson, ibid.
9. I. R. Lindemuth, ibid.
10. S. I. Braginskii, Sov. Phys. JETP 6, 494 (1958).
11. M. G. Haines, Proc. Phys. Soc. London 76, 250 (1960).
12. W. H. Bennett, Phys. Rev. 45, 890 (1934).
13. L. Spitzer, Physics of Fully Ionized Gases, Interscience, New York, 1962.
14. To be precise, it has been well known for decades that the growth rate is of the order of kv_A, but exact growth rates from ideal MHD for diffuse profiles have recently been calculated by M. Coppins, Plasma Phys. and Controlled Fusion 30, 201 (1988).
15. R. J. Tayler, Rev. Mod. Phys. 32, 907 (1960).
16. M. Coppins, I. D. Culverwell, and M. G. Haines, Phys. Fluids 31, 2688 (1988).
17. P. Rosenau, R. A. Nebel, and H. R. Lewis, Phys. Fluids (in press).

18. S. Lundquist, Ark. Fys. 5, 297 (1952).

19. I. R. Lindemuth, G. H. McCall, and R. A. Nebel, Phys. Rev. Lett. 62, 264 (1989).

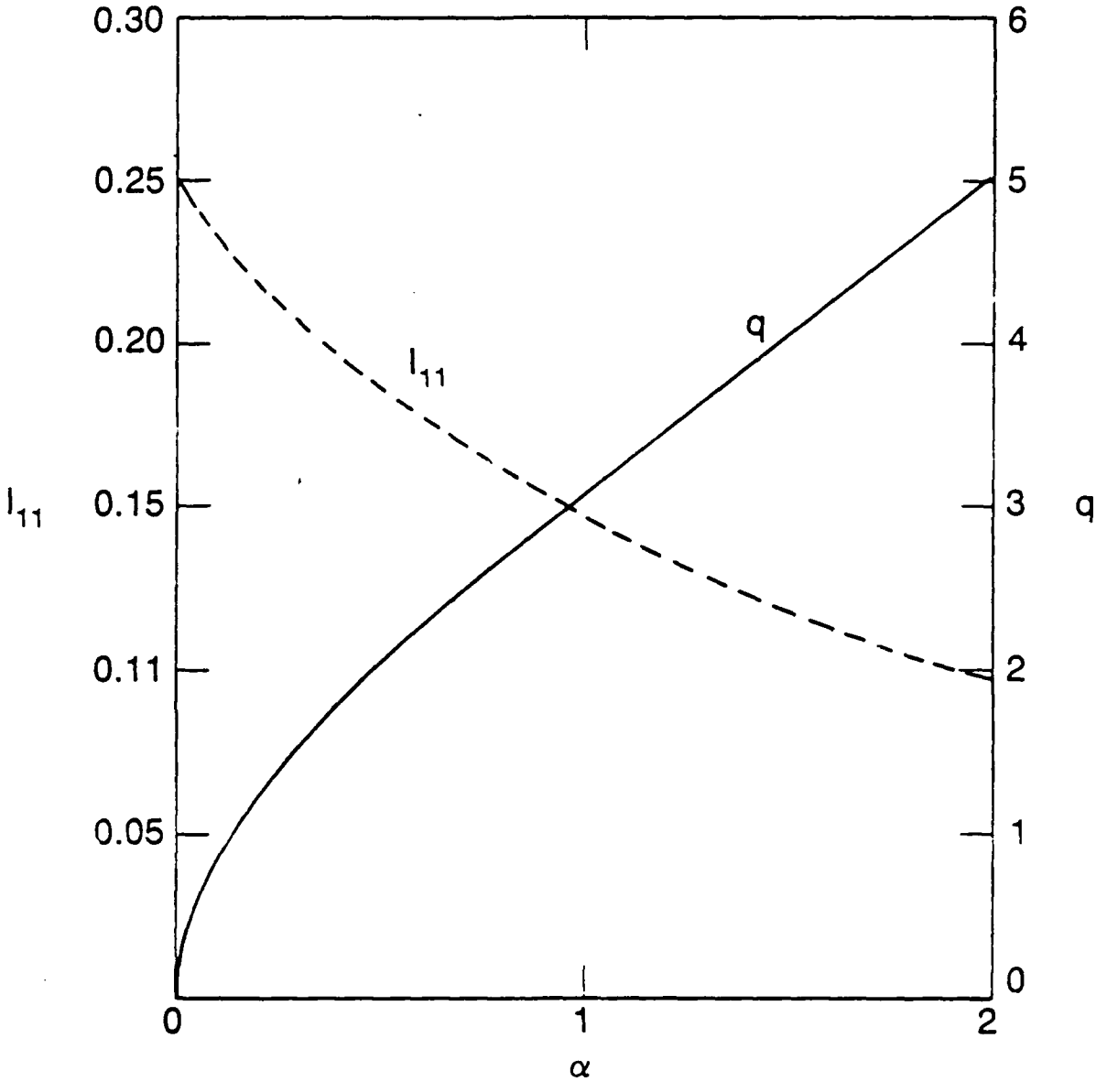

Fig. 1. The function $I_{11}(\alpha)$ defined in Eqs. (47) is shown as the dashed curve, using the scale at left. The function $q(\alpha)$, from Eq. (18) is shown as the solid curve, using the scale at right.

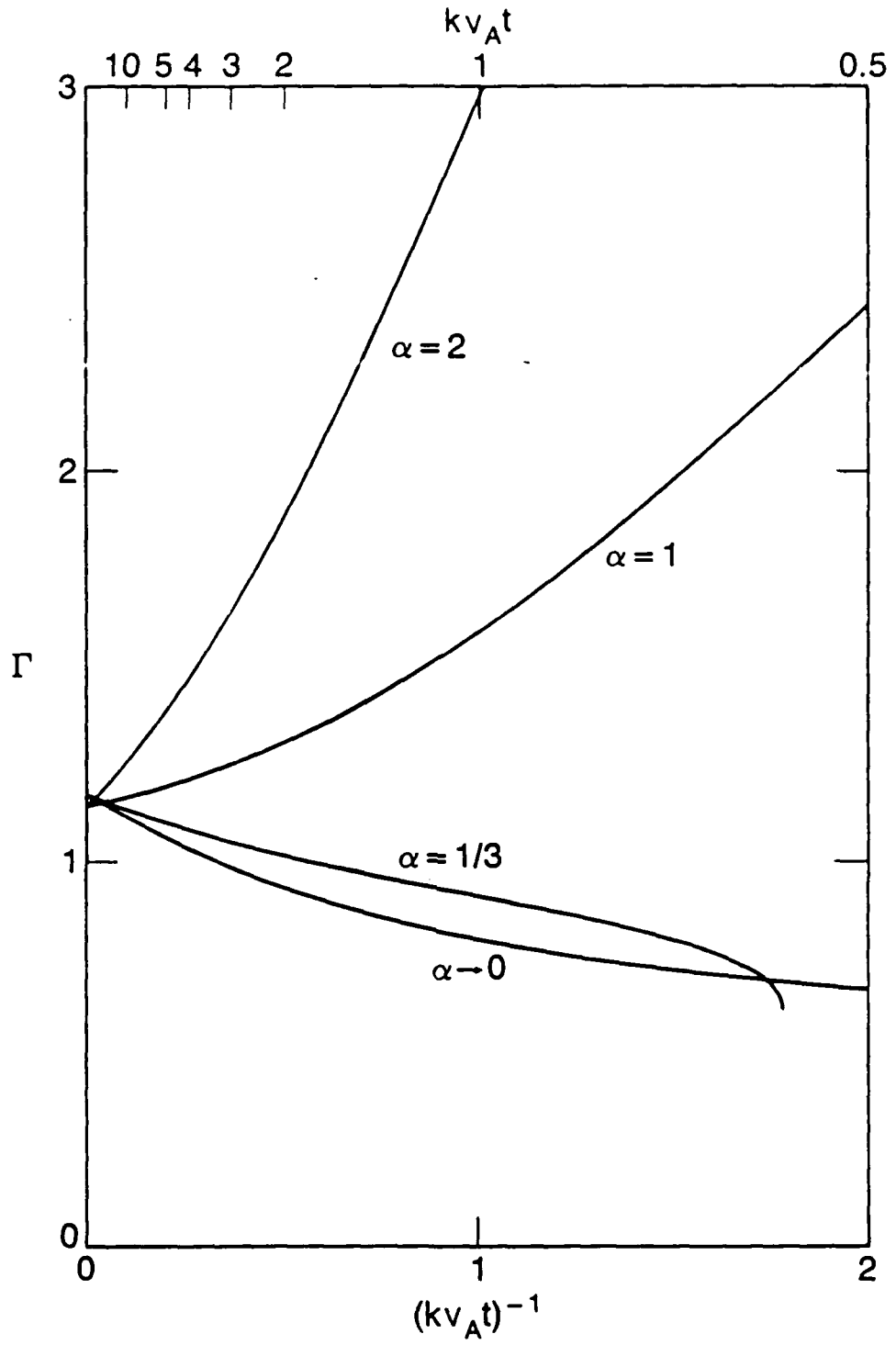

Fig. 2. The instability growth rate Γ [normalized to kv_A, where the Alfven speed v_A is defined in Eq. (43)], for four different values of the parameter α, which specifies the time dependence of the current. Note that the value of Γ for $\alpha = 1/3$ becomes complex for $(kv_At)^{-1} > (kv_At^*)^{-1} \simeq 1.8$.

Distribution List*

Naval Research Laboratory
4555 Overlook Avenue, S.W.
Attn: CAPT J. J. Donegan, Jr. - Code 1000
Dr. M. Lampe - Code 4792 (20 copies)
Dr. T. Coffey - Code 1001
Head, Office of Management & Admin - Code 1005
Deputy Head, Office of Management & Admin - Code 1005.1
Directives Staff, Office of Management & Admin - Code 1005.6
Director of Technical Services - Code 2000
ONR - Code 0124
NRL Historian - Code 2604
Dr. W. Ellis - Code 4000
Dr. S. Ossakow - Code 4700 (26 copies)
B. Pitcher - Code 4790A
Library - Code 2628 (22 copies)
D. Wilbanks - Code 2634

* Every name listed on distribution gets one copy except for those where extra copies are noted.

Dr. John P. Apruzese
Naval Research Laboratory
Plasma Radiation Branch
Code 4720
Washington, DC 20375

Dr. John F. Benage, Jr.
Los Alamos National Laboratory
MS-E526
Los Alamos, NM 87545

Dr. Ekkehard P. Boggasch
University of Maryland
Laboratory for Plasma Research
College Park, MD 20742

Dr. Thomas J. Burgess
Sandia National Laboratories
Division 1261
P.O. Box 5800
Albuquerque, NM 87185

Dr. Frederick L. Cochran
Berkeley Research Associates, Inc.
P.O. Box 852
Springfield, VA 22150

Dr. Denis G. Colombant
Naval Research Laboratory
Code 4790
Washington, DC 20375

Dr. Jack Davis
Naval Research Laboratory
Plasma Radiation Branch
Code 4720
Washington, DC 20375-5000

Dr. Christophr Deeney
Physics International
2700 Merced Street
San Leandro, CA 94577

Dr. James H. Degnan
Air Force Weapons Laboratory
Kirtland AFB, NM 87117

Dr. William F. Dove
Advanced Fusion Concepts Brnch
Div. of Applied Plasma Physics
Office Fusion Energy/ER-543-GTN
U.S. Department of Energy
Washington, DC 20545

Dr. Shimon Eckhouse
Maxwell Laboratories, Inc.
9244 Balboa Avenue
San Diego, CA 92123

Dr. Carl Ekdahl
Los Alamos National Laboratory
P.O. Box 1663
Mail Stop D410
Los Alamos, NM 87545

Dr. Franklin S. Felber
JAYCOR
11011 Torreyana Road
P.O. Box 85154
San Diego, CA 92138

Dr. Michael Finkenthal
Johns Hopkins University
Dept. of Physics & Astronomy
Rowland Hall
Baltimore, MD 21218

Dr. Amnon Fisher
University of California, Irvine
Physics Department
Irvine, CA 92717

Mr. Kent A. Gerber
Naval Research Laboratory
Code 4760
Washington, DC 20375-5000

Ms. Miriam Gersten
Maxwell Laboratories, Inc.
8888 Balboa Avenue
San Diego, CA 92123

Dr. John L. Giuliani
Naval Research Laboratory
Plasma Radiation Branch
Plasma Physics Division
Code 4720
Washington, DC 20375

Dr. Alan H. Glasser
Los Alamos National Laboratory
CTR-6 Group
Mail Stop F-642
P.O. Box 1663
Los Alamos, NM 87545

Dr. Arthur E. Greene
Los Alamos National Laboratory
Xx-10, MS B259
Los Alamos, NM 87545

Dr. Hans R. Griem
University of Maryland
Lab for Plasma Research
Energy Research Building
College Park, MD 20742

Dr. Jay E. Hammel
Los Alamos National Laboratory
P.O. Box 1663
CTR-8, MS K639
Los Alamos, NM 87545

Dr. Charles W. Hartman
Lawrence Livermore National Lab.
P.O. Box 808
L-637
Livermore, CA 94550

Dr. David D. Hinshelwood
Naval Research Laboratory
Code 4773
Washington, DC 20375-5000

Dr. Warren W. Hsing
Sandia National Laboratories
P.O. Box 5800
Albuquerque, NM 87185

Dr. Thomas W. Hussey
Sandia National Laboratories
P.O. Box 5800
Albuquerque, NM 87185

Dr. Franz Jahoda
Los Alamos National Laboratory
P.O. Box 1663
CTR-8, MS K639
Los Alamos, NM 87545

Dr. Robert A. Krakowski
Los Alamos National Laboratory
CTR-12, MSF641
P.O. Box 1663
Los Alamos, NM 87545

Dr. Mahadevan Krishnan
Physics International
2700 Merced Street
San Leandro, CA 94577-0599

Dr. M. Kristiansen
Texas Tech University
Dept. of Electrical Engineering
Lubbock, TX 79409-4439

Dr. Martin Lampe
Naval Research Laboratory
Code 4792
Washington, DC 20375

Mr. P. David LePell
Physics International Company
2700 Merced Street
San Leandro, CA 94577

Dr. Jae K. Lee
General Atomics (13-318)
P.O. Box 85608
San Diego, CA 92138

Dr. Irvin R. Lindemuth
Los Alamos National Laboratory
Applied Theoretical Physics Div.
MS-E531
P.O. Box 1663
Los Alamos, NM 87545

Dr. Nicholas G. Loter
Maxwell Laboratories, Inc.
8888 Balboa Avenue
San Diego, CA 92123

Dr. Ralph H. Lovberg
Los Alamos National Laboratory
P.O. Box 1663
CTR-8, MS K639
Los Alamos, NM 87545

Dr. Rodney J. Mason
Los Alamos National Laboratory
X-1, MS-E531
Los Alamos, NM 87545

Stephen M. Matthews
Lawrence Livermore National Lab.
L-389, Box 808
Livermore, CA 94550

Dr. Keith. Matzen
Sandia National Laboratories
Code 1273
P.O. Box 5800
Albuquerque, NM 87185

George H. Miley
University of Illinois
214 Nuclear Engr Lab
103 S. Goodwin Avenue
Urbana, IL 61801

Cornelius A. Morgan
University of Maryland
Plasma Spectroscopy Group
Building #223
College Park, MD 20742

Dr. David Mosher
Naval Research Laboratory
Code 4770.1M
Washington, DC 20375

Dr. V. Nardi
Stevens Institute of Technology
Hoboken, NJ 07803

Dr. Thomas Nash
Physics International Co.
2700 Merced Street
San Leandro, CA 94577

Dr. Richard A. Nebel
Los Alamos National Laboratory
MS F642
Los Alamos, NM 87545

Dr. Nino R. Pereira
Berkeley Research Associates, Inc.
P.O. Box 852
Springfield, VA 22150

Dr. Joseph D. Perez
Auburn University
Physics Department
206 Allison Lab
Auburn University, AL 36849-5311

Dr. Darrell L. Peterson
Los Alamos National Laboratory
MS B259
Los Alamos, NM 87545

Dr. John L. Porter
Sandia National Laboratories
P.O. Box 5800
Albuquerque, NM 87185

Dr. Charles Powell
Stevens Institute of Technology
Dept. of Physics
Hoboken, NJ 07030

Mr. Rahul Prasad
Yale University
Mason Lab.
9 Hillhouse Avenue
New Haven, CT 06520

Dr. Peter E. Pulsifer
Berkeley Research Associates, Inc.
P.O. Box 852
Springfield, VA 22150-0852

Dr. Niansheng Qi
Laboratory of Plasma Studies
Cornell University
369 Upson Hall
Ithaca, NY 14853

Dr. John C. Riordan
Physics International Co.
2700 Merced Street
San Leandro, CA 94577

Dr. William Rix
Maxwell Laboratories, Inc.
8888 Balboa Avenue
San Diego, CA 92123

Charles W. Roberson
Office of Naval Research
Physics Division, Code 1112
800 North Quincy St.
Arlington, VA 22308

Dr. Anthony E. Robson
Naval Research Laboratory
Code 4760
4555 Overlook Ave., SW
Washington, DC 20375

Professor Norman F. Roderick
University of New Mexico
Dept. Chemical & Nuclear Eng
Albuquerque, NM 87131

Dr. Norman Rostoker
University of California, Irvine
Physics Department
Irvine, CA 92717

Dr. Gary A. Saenz
Rockwell International
Rocketdyne Division
6633 Canoga Ave.
M/S: FA03
Canoga Park, CA 91303

Dr. David W. Scudder
Los Alamos National Laboratory
P.O. Box 1663
MS K639
Los Alamos, NM 87545

Dr. John D. Sethian
Naval Research Laboratory
Code 4762
4555 Overlook Ave., SW
Washington, DC 20375

Dr. Jack S. Shlachter
Los Alamos National Laboratory
CTR-8, MS K639
P.O. Box 1663
Los Alamos, NM 87545

Dr. Rick B. Spielman
Sandia National Laboratories
P.O. Box 5800
Albuquerque, NM 87115

Dr. Stavros Stephanakis
Naval Research Laboratory
Code 4773
4555 Overlook Avenue, S.W.
Washington, DC 20375-5000

Dr. Leaf Turner
Los Alamos National Laboratory
CTR-6, MS F642
P.O. Box 1663
Los Alamos, NM 87545

Dr. Han S. Uhm
Naval Surface Warfare Center
R-41
White Oak
Silver Spring, MD 20903-5000

Dr. Kenneth D. Ware
Maxwell Laboratories
8888 Balboa Avenue
San Diego, CA 92123

Dr. Frank J. Wessel
University of California, Irvine
Physics Department
Irvine, CA 92717

Dr. Kenneth G. Whitney
Naval Research Laboratory
Plasma Radiation Branch
Code 4720
4555 Overlook Avenue, SW
Washington, DC 20375

Dr. Andrew R. Wilson
S-Cubed
A Division of Maxwell Laboratories
PO Box 1620
La Jolla, CA 92038

Dr. Gerold Yonas
Titan Technologies
9191 Towne Centre Dr.
Suite 600
San Diego, CA 92122

Dr. Frank C. Young
Naval Research Laboratory
Code 4770.1
Washington, DC 20375-5000

Naval Research Laboratory
Washington, DC 20375-5000
Code 1220

Do NOT make labels
for these two-below:
Records---(1 copy)

Director of Research
U.S. Naval Academy
Annapolis, MD 21402
(2 copies)

Naval Research Laboratory
Washington, DC 20375-5000
Code 2630
Timothy Calderwood